Int. J. Electrochem. Sci., 16 **(2021)** Article Number: 21129, doi: 10.20964/2021.12.46

International Journal of
ELECTROCHEMICAL
SCIENCE
www.electrochemsci.org

Short Communication

Research on the Mechanism of Sediment Formation of Al Compounds on Platinum Electrodes in Inner Water Cooling Systems for HVDC Converter Valves

Zeming Yang[1], Daoyu Li[2], Xuezhong Liu[3,], Baihao Gong[3], Xiuying Jiao[4], Shicai Lu[2], Chenxing Wang[3], Yi Jiang[2], Huaping Xu[2], Yi Chen[2]*

[1] China Southern Power Grid Company Limited, Guangzhou 510623, China
[2] Guiyang Bureau, Extra High Voltage Power Transmission Company, China Southern Power Grid Company Limited, Guiyang 550081, China
[3] State Key Laboratory of Electrical Insulation and Power Equipment, Xi'an Jiaotong University, Xi'an 710049, China
[4] Xi'an XD Power Systems Company Limited, China XD Group, Xi'an 710075, China
[*]E-mail: xliu@xjtu.edu.cn

Received: 21 July 2021 / *Accepted:* 8 October 2021 / *Published:* 10 November 2021

The reliable operation of high voltage direct current (HVDC) converter valves is threatened by the problem of sediment deposition on platinum electrodes in inner water cooling systems. In this paper, simulated corrosion experiments of aluminium heat sinks and simulated deposition on pin-type platinum electrodes were carried out in the laboratory. Based on thermodynamic theory, the existing forms of Al(III) species in cooling water were revealed through theoretical calculations. According to the electrophoretic deposition, the sediment deposition process on the platinum electrodes was numerically simulated by COMSOL software simulation. The research results show that the pH value has a great influence on the existing forms of Al(III) species in cooling water. More importantly, the electrical properties of aluminum reaction species in inner valve cooling systems are dominated by environmental pH values rather than the original corrosion reactions, thus leading to the phenomenon that sediment depositions are found only on platinum electrodes connected as anodes in engineering practice. Both the simulated experiments and the numerical calculation also indicate that the deposited sediment on the platinum electrode is rod-shaped and that the growth rate of sediment thickness decreases with time. This research can play an important role in clarifying the phenomenon and mechanism of deposition on platinum electrodes in HVDC converter valves.

Keywords: HVDC, Converter valve, Cooling system, Platinum electrodes, Sediment deposition

1. INTRODUCTION

High voltage direct current (HVDC) power transmission has been used for long-distance bulk-power delivery, asynchronous AC system interconnections and the integration of remote large scale renewable sources into the system [1–2]. As the core equipment of the HVDC transmission system, the converter valve generates considerable heat during normal operation. Once the junction temperature of large power thyristors in the converter valve excessively exceeds the specified value, device failure will probably occur. Therefore, valve cooling systems are designed to remove excess heat in time. Deionized water qualifies for the coolant of valve cooling systems because of its excellent characteristics of low viscosity, electrical insulation and high heat transfer capability [3–4]. To avoid corrosion of aluminium heat sinks caused by leakage current in the cooling water, pin-type platinum electrodes, E_1~E_4 as shown in Figure 1, were applied in engineering practice to make the electrical potential in the distributed water circuit (or pipe) consistent with the electrical potential in the corresponding electrical circuit. However, the emergence of another simultaneous problem, that is, sediment deposited on platinum electrodes, which will cause blockage of the water circuit and limit the primary function of the cooling system and platinum electrodes, has seriously threatened the normal operation of converter valves for many years [5].

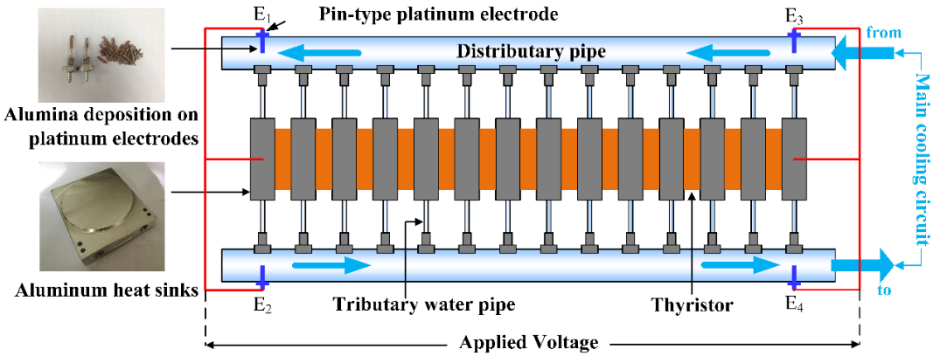

Figure 1. Diagram of the typical structure of distributed water circuits in a converter valve unit

To solve above problem, related scholars have carried out extensive research mainly from three aspects. First, some scholars have investigated the source of sediment deposition. Li [6] found that sediment deposition consisted mainly of mixed aluminium oxides and hydroxides (alumina), which indicated that aluminum heat sinks still suffer from electrolytic corrosion despite the installation of platinum electrodes. This viewpoint was later demonstrated by Wang [8–10], who also found that the anodic or cathodic leakage current through aluminium heat sinks will lead to stray-current corrosion or alkaline corrosion, respectively. Second, the deposition mechanism of the platinum electrodes was partly revealed. Wang [7,11] found that the degree of deposition was determined by the directions and magnitude of the electrical currents through the electrodes. Weber [12] proposed a field accumulation model and combined the proton tunneling effect to explain the mechanism of the alumina deposition process. Based on electrochemical deposition, Gao and Song [13–14] simulated the sediment deposition process by a coupling model. Finally, some antideposition methods were proposed. Weber proposed a method of injecting CO_2 to prevent the formation of deposition [12]. Wang designed an antideposition

device that can compete with the deposition process on pin-type platinum electrodes [15]. Moreover, some scholars [16–18] studied some factors affecting the corrosion rate of aluminium electrodes, which provided guidance for inhibiting the corrosion reactions of heat sinks at the source.

However, current studies lack reasonable explanations for the deposition phenomenon of platinum electrodes in valve cooling systems, especially for the fact that the alumina deposition tends to deposit on the platinum electrodes connected as anodes. They generally think that the electrolytic corrosion of heat sinks in valve cooling systems will just produce aluminate $Al(OH)_4^-$, and then $Al(OH)_4^-$ will migrate to anodes by Coulomb force. However, our previous work has pointed out that the electrolytic corrosion of aluminium heat sinks will also produce Al^{3+}, which indicates that there should also be sediment deposition on the platinum electrodes connected as cathodes. Consequently, it is significant to further develop the mechanism of sediment formation of Al compounds on the platinum electrodes to explain the deposition phenomenon for valve cooling systems in engineering practice.

In this paper, a simulated deposition experiment was conducted to explore the deposition mechanism of platinum electrodes in the laboratory, and a numerical simulation model based on electrophoretic deposition was also established to explore the deposition mechanism. Moreover, the effect of pH on the existing forms of aluminium reaction species was analysed according to the thermodynamic calculations and simulated corrosion and deposition experiments.

2. EXPERIMENTAL

2.1. Simulated deposition experiment

To explore the deposition mechanism of platinum electrodes, a simulated electrode deposition setup was established in the laboratory, as shown in Figure 2. The distributary cooling water pipes were made of polymethyl methacrylate, and five pin-type platinum electrodes were mounted along water pipes. The electrodes of E_3 and E_5 are cathodes, and the electrodes of E_1, E_2 and E_4 are anodes. In addition, the applied voltage should make the current through the surface of electrodes consistent with that the electrical current of the valve cooling system in engineering practice, which is approximately 4 mA. As is apparent in Figure 3, and the electrical current through the surface of electrodes E_1, E_3, E_4 and E_5 was held from 3 to 4 mA, and the current through the surface of electrode E_2 was held at 0.5 to 0.6 mA.

The designed experimental setup was connected to the simulated valve cooling system, in which the aluminium heat sinks suffer from electrolytic corrosion under simulated conditions. To accelerate the deposition rate of electrodes, the simulated valve cooling system in the laboratory was operated for 600 hours before the simulated deposition experiment started. Table 1 presents the quality parameters of circulating water. The high concentration of ferric ions in circulating water might be caused by the corrosion of stainless-steel pipes in the simulated valve cooling system. Since the experiment was carried out in a nonsealed environment, the dissolution of CO_2 in the ambient air could make the pH value of the circulating water weakly acidic.

Table 1. Initial quality parameters of circulating water in the simulated deposition experiment

Temperature (°C)	Water flux (L/h)	Conductivity (μS/cm)	pH	Dissolved oxygen content (mg/L)	$c(Al)_t$ (μg/L)	$c(Fe)_t$ (μg/L)
25	1600	4.0	6.15	2.5	210.0	51.0

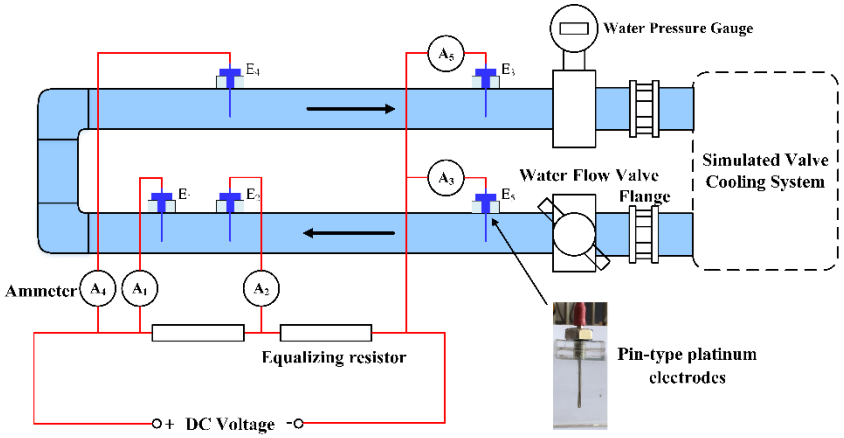

Figure 2. Schematic diagrams of simulated electrode deposition setups

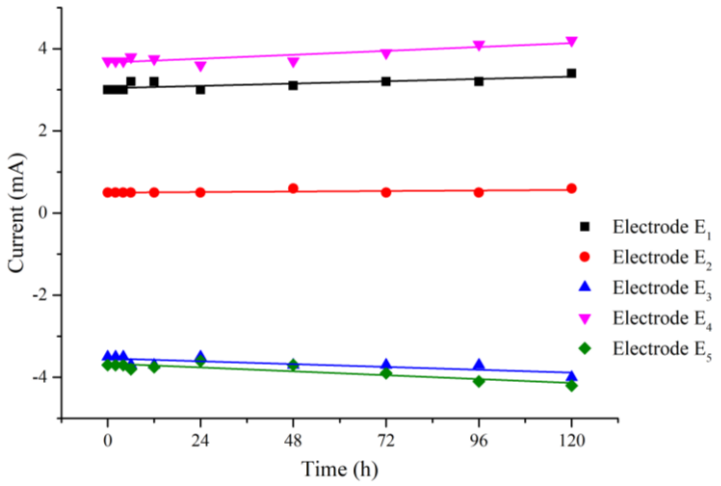

Figure 3. Electric current through anodes and cathodes respectively: E_1, E_2 and E_4 are platinum anodes, E_3 and E_5 are platinum cathodes

2.2. Simulated corrosion and deposition experiments

To verify that the electrical properties of aluminium reaction species are either determined by the quality parameters of the solution (especially pH) or corrosion reactions of aluminium sinks at the source, simulated experiments of combined corrosion with deposition were conducted in two separated water cell setups. Diagrams of the simulated corrosion and deposition setup are shown in Figure 4. Figure 4 (a) shows the simulated corrosion of anode and deposition experiments, and Figure 4 (b) shows the simulated corrosion of cathode and deposition experiments. The difference between the two

experimental setups is the polarity of the applied voltage, which will produce different aluminium corrosion products from the headstream with opposite electrical properties. Three sheet samples made of aluminium alloy whose sizes were all 70 mm×10 mm×2 mm were used to simulate the corrosion process of aluminium heat sinks in converter valves. Each sample was polished with abrasive papers from 200 to 800 meshes per linear inch before the experiment. The immersion depth of each sheet sample was maintained at 40 mm during the experiment. Moreover, two pin-type platinum electrodes whose immersion depth was maintained at 23 mm were placed opposite to the sheet samples. Deionized water was used as supplementary water.

The experiment was divided into two stages, and each stage lasted for a total of 240 hours. In stage I, switch S_1 was closed, and S_2 was opened. To accelerate the electrolytic corrosion rates of aluminum sheet samples, the surface current density of the aluminium sheet sample was maintained at 2.0 μA/mm^2, which is ten times as much as the average current density of the current concentrated distribution area of heat sinks in engineering practice [8]. In stage II, the current through the electrode was held from 3 to 4 mA, which is equal to the current through platinum electrodes in engineering practice. The changes in the quality parameters of circulating water are listed in Table 2. Since all the experiments were carried out in a nonsealed environment, the dissolution of CO_2 in air could decrease the pH value of water.

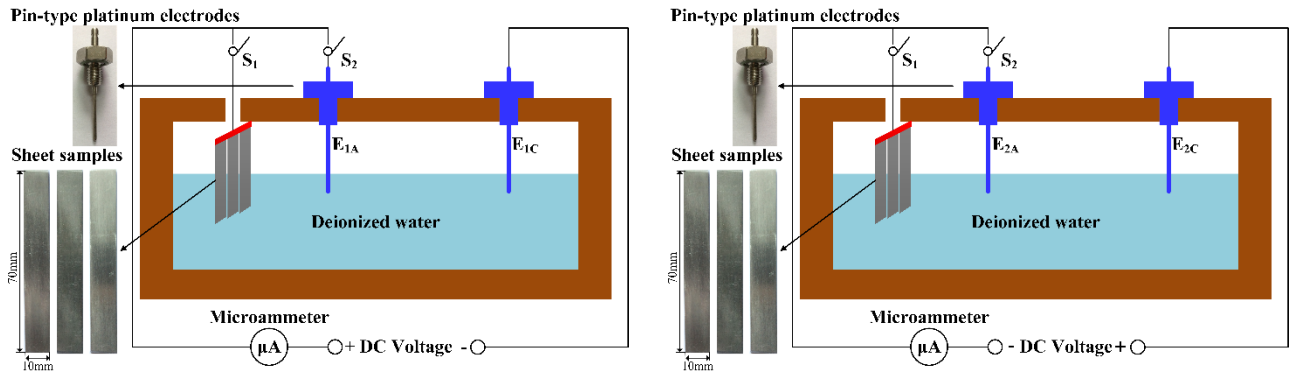

(a) Corrosion of anode and deposition (b) Corrosion of cathode and deposition

Figure 4. Schematic diagrams of simulated corrosion and deposition setups

Table 2. Quality parameters of circulating water before and after simulated corrosion and deposition experiments

Experimental devices \ Water quality parameters		Temperature (°C)	Conductivity (μS/cm)	Dissolved oxygen content (mg/L)	pH
Corrosion of anode and deposition	Initial	25.0	0.45	2.0	6.78
	Final	26.8	4.88	2.8	6.01
Corrosion of cathode and deposition	Initial	25.0	0.45	2.0	6.78
	Final	29.0	4.73	3.1	5.95

2.3. Theoretical calculation for distribution ratios of Al(III) species

Aluminium ion, Al^{3+}, will convert into various Al(III) species with H_2O and OH^- in water. Various hydrolysis reactions of Al^{3+} in water and their equilibrium constants are given in Table 3.

Table 3. Equilibrium constants of various hydrolysis reactions of Al^{3+} at 25 °C [19–20] and 50 °C

Hydrolysis reactions	log K, 25 °C	log K, 50 °C
$Al^{3+}+H_2O \rightarrow Al(OH)^{2+}+H^+$	-5.52/-5.0	-4.78/-4.26
$Al^{3+}+2H_2O \rightarrow Al(OH)_2{}^{+}+2H^+$	-8.71/-10.1/-11.3	-7.17/-8.56/-9.76
$Al^{3+}+3H_2O \rightarrow Al(OH)_3(aq)+3H^+$	-16.0	-13.92
$Al^{3+}+3H_2O \rightarrow Al(OH)_3(am)+3H^+$	-10.4	-8.77
$Al^{3+}+4H_2O \rightarrow Al(OH)_4^- + 4H^+$	-23.46	-20.82
$2Al^{3+}+2H_2O \rightarrow Al_2(OH)_2{}^{4+}+2H^+$	-6.3	-4.98
$3Al^{3+}+4H_2O \rightarrow Al_3(OH)_4{}^{5+}+4H^+$	-13.57/-13.74	-11.50/-11.64
$6Al^{3+}+15H_2O \rightarrow Al_6(OH)_{15}{}^{3+}+15H^+$	-47.00	-39.83
$7Al^{3+}+17H_2O \rightarrow Al_7(OH)_{17}{}^{4+}+17H^+$	-48.80/-59.48	-41.36/-50.41
$8Al^{3+}+20H_2O \rightarrow Al_8(OH)_{20}{}^{4+}+20H^+$	-68.70	-58.22
$13Al^{3+}+28H_2O \rightarrow Al_{13}O_4(OH)_{24}{}^{7+}+32H^+$	-97.6	-80.94

The hydrolysis equilibrium constants at 50 °C are calculated based on the Van't Hoff equation and the equilibrium constants at 25 °C.

The distribution ratio, α, is defined as the percentage of aluminum concentration in the designated Al(III) species divided by the overall concentration of dissolved Al(III) as $c(Al)_t$.

The material balance equation of the Al-H_2O solution system could be derived in the forms below if the formation of precipitation $Al(OH)_3$ (am) was not considered.

$$c(Al)_t = [Al^{3+}]+[Al(OH)^{2+}]+[Al(OH)_2{}^{+}]+[Al(OH)_3(aq)]+2\cdot[Al_2(OH)_2^{4+}]+3\cdot[Al_3(OH)_4{}^{5+}] +6\cdot[Al_6(OH)_{15}{}^{3+}]+7\cdot[Al_7(OH)_{17}{}^{4+}]+8\cdot[Al_8(OH)_{20}{}^{4+}]+13\cdot[Al_{13}O_4(OH)_{24}{}^{7+}] \quad (1)$$

$$-1+(1+10^{pH-5}+10^{2pH-10.1}+10^{3pH-16}+10^{4pH-23.46})\alpha_0+2\cdot c(Al)_t\cdot 10^{2pH-6.3}\cdot\alpha_0{}^2+ 3\cdot c(Al)_t^2\cdot 10^{4pH-13.57}\cdot\alpha_0{}^3+6\cdot c(Al)_t^5\cdot 10^{15pH-47}\cdot\alpha_0^6+7\cdot c(Al)_t^6\cdot 10^{17pH-48.8}\cdot\alpha_0^7+ 8\cdot c(Al)_t^7\cdot 10^{20pH-68.7}\cdot\alpha_0^8+13\cdot c(Al)_t^{12}\cdot 10^{32pH-97.6}\cdot\alpha_0^{13}=0 \quad (2)$$

where α_0 is the concentration of Al^{3+} divided by $c(Al)_t$.

2.4 Theoretical analysis of deposition model

The sediment deposition process on platinum electrodes is simulated based on electrophoretic deposition. The mass of sediment per unit area is calculated by the following expression when the electrode current is used for the water electrolysis reaction.

$$m = \frac{C_i}{n_i}\frac{i_{loc}t}{Z_i e} \tag{3}$$

where C_i is the mass of charged colloidal particles contained in a unit volume of solution; i_{loc} is normal current density of electrode surface; t is the time of applied current; n_i represents the number of colloidal particles per unit volume in solution; Z_i stands for the number of charged colloidal particles, and e is unit charge.

In addition, the current distribution in the water circuit should follow both the Ohm law and charge conservation law.

$$i_1 = -\sigma \nabla \varphi \tag{4}$$

$$\nabla i_1 = 0 \tag{5}$$

where i_1 is the current density; σ is the conductivity of ultrapure water; and φ is the electrical potential in the waterway.

If other impurity colloidal particles are ignored, the relationship between the conductivity of deionized water and the drift mobility of charged ions is shown as follows:

$$\sigma = n_i(Z_i e)\mu \tag{6}$$

where μ is drift mobility of charged ions in water.

For the electrophoresis of a spherical particle with a small radius of curvature, the drift mobility is connected with the ζ potential of the charged particles.

$$\mu = \frac{2\varepsilon_0 \varepsilon_r \zeta}{3\eta} \tag{7}$$

where ε_0 is the permittivity of a vacuum; ε_r is the relative dielectric constant of the medium; and η is the viscosity of the colloidal system.

Moreover, the total concentration of aluminium reaction species of the reaction zone, conductivity, flow field parameters and some other environmental parameters are assumed to remain constant when the corrosion rate of heat sinks and the deposition rate of the platinum electrodes reach an equilibrium state.

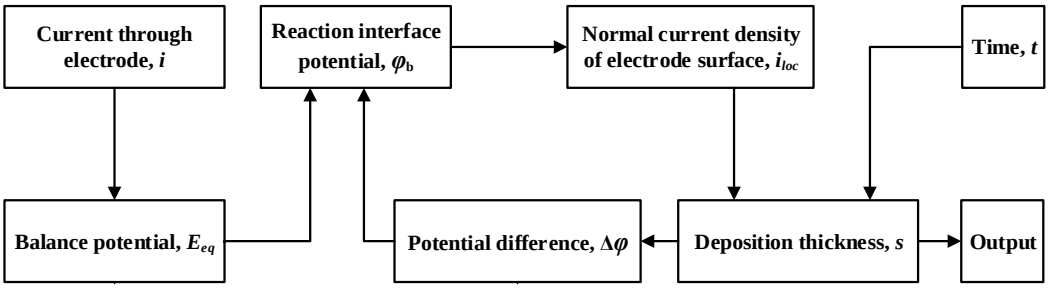

Figure 5. Flow chart of simulated deposition calculation

The flow chart of the simulated deposition calculation is shown in Figure 5. In Figure 5, φ_b represents the potential of the outer surface of sediment deposition, E_{eq} represents the balance potential and is determined by the current through the electrode, $\Delta\varphi$ represents the potential difference between the outer surface of the deposition and the inner surface of the deposition, and s represents the deposition

thickness. The relationship between the growth of each deposition layer thickness and the time is calculated by meshing the surface of the pin-type platinum electrode. Finally, the thickness growth of the deposition on the electrode surface is output.

3. RESULTS AND DISCUSSION

3.1. Dominant factors determined electrical properties of aluminium reaction species

In the simulated deposition experiment, as shown in Figure 6, there was almost no sediment deposition on the surface of anodes E_1 and E_4 whereas the sediment deposition could evidently be observed on the surface of cathodes E_3 and E_5. Furthermore, there was no sediment deposition on the E_2-E_3 surface, which refers to the surface of electrode E_2 that facing cathode E_3. However, a small amount of sediment was deposited on the E_2-E_1 surface, which refers to the surface of electrode that facing E_1. The chemical composition of the sediment deposition was analysed by energy dispersive spectrometer (EDS) after the experiment, as presented in Table 4. Al and Fe are the main metal element in the experimental samples, and the chemical composition is similar to the industrial samples [7]. The difference is that the content of Fe is high in experimental samples. The explanation is that the stainless-steel pipes in the simulated valve cooling system suffers from electrolytic corrosion, thus producing Fe ions in the circulating water. Since the sediment is crimson, as shown in Figure 6, it can be inferred that Fe ions could take part in the reactions on the platinum electrodes and forms Fe_2O_3.

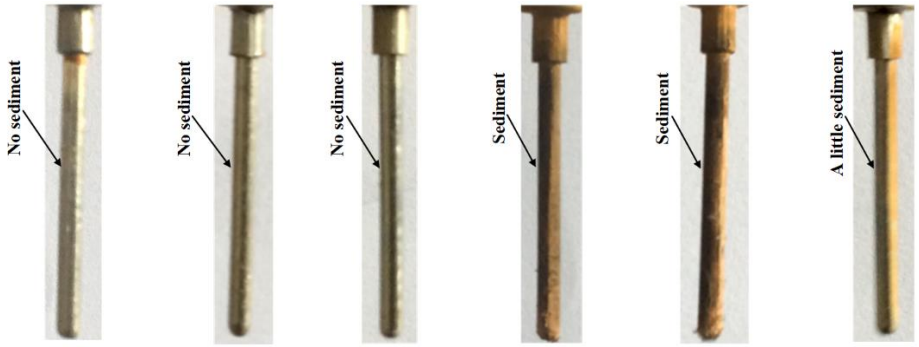

(a) Anode E_1; (b) Anode E_4; (c) E_2-E_3 surface; (d) Cathode E_3; (e) Cathode E_5; (f) E_2-E_1 surface

Figure 6. Surface morphology of electrodes after simulated deposition experiment

Table 4. Atomic fraction and weight fraction of sediment deposition samples in the simulated deposition experiment

Electrodes / Elements	Cathode E_3		Cathode E_5		Cathode surface of E_2	
	Wt (%)	At (%)	Wt (%)	At (%)	Wt (%)	At (%)
O	38.32	63.42	47.81	69.70	41.57	67.39
Al	14.23	13.96	12.51	10.81	8.64	8.30
Fe	47.26	22.43	34.32	14.35	57.87	22.25
Mg	0.002	0.20	0.05	5.14	0.02	2.05

Apparently, the experimental result seems contrary to the deposition phenomenon in engineering practice, where the sediment deposition on the platinum electrodes connected as anodes was thicker. How to explain this contradiction? Current studies have reached a consensus on the sources of alumina depositions, which are the corrosion products of aluminium heat sinks in valve cooling systems. Our previous work found that an electric leakage up to 10.8 μA was conducted through the heat sinks from/to one tributary water pipe, thus leading to the electrolytic corrosion of heat sinks, the corrosion reactions are shown as follows [8]:

$$Al - 3e^- \rightarrow Al^{3+} \quad (8)$$

$$2Al + 2OH^- + 6H_2O \rightarrow 3H_2 \uparrow + 2Al(OH)_4^- \quad (9)$$

The reactions of aluminium heat sinks will produce aluminum corrosion products (Al^{3+}, $Al(OH)_4^-$) with opposite electrical properties at the source. Furthermore, the current studies have reached another consensus that the migration direction of aluminium reaction species in circulating water is determined by the electric field. However, the deposition phenomenon in both simulated deposition experiment and engineering practice illustrates that there should be many aluminium reaction species with the same electrical properties in circulating water, indicating that the electrical properties of the aluminium corrosion products might change when they migrate to the platinum electrodes. The environmental parameters of circulating water, especially the pH value, seemed to be an important factor that could change the electrical properties of the corrosion products when they migrate to the platinum electrodes [15]. Since both the corrosion reactions of aluminum heat sinks and the environmental parameters of circulating water may determine the electrical properties of the aluminum reaction species, simulated corrosion and deposition experiments was conducted in the laboratory.

The results of simulated corrosion and deposition experiments are shown in Figure 7. For the simulated corrosion of the anode and deposition experiments, the surface of cathode E_{1C} absorbed some white substance, and some visible flocculent sediments gathered around the electrode at the end of stage I. At the end of stage II, there was no sediment deposited on anode E_{1A}, and it could be still observed that there was sediment deposited on electrode $E_{1C.}$ For the simulated corrosion of cathode and deposition experiments, almost no sediment was deposited on anode E_{2A} at the end of stage I. However, sediment was deposited on cathode E_{2C} compared to stage II. Moreover, no sediment deposition was observed on anode E_{2A}. The chemical composition of sediment deposition on electrodes was analysed by EDS after the experiments. The sediment deposition on the cathode consisted primarily of mixed alumina (oxides, hydroxides), which was comparable to industrial samples.

If the electrical properties of aluminium reaction species had been determined by the corrosion reactions generated at the source, $Al(OH)_4^-$ generated by alkaline corrosion would have deposited on anode E_{2A}. There would have been no sediment depositing on cathode E_{2C} either. However, it is still too early to draw the conclusion that the electrical properties of aluminum reaction species are determined by the pH value rather than the corrosion reactions of aluminum heat sinks. Quantitative calculations are still required to further reveal the effect of the pH value on the existing forms of Al(III) species.

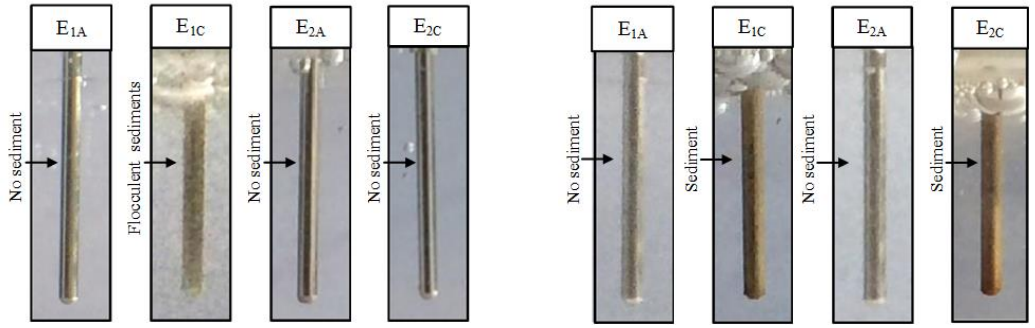

(a) at end of Stage I (corrosion stage) (b) at end of Stage II (deposition stage)

Figure 7. Changes of surface morphology of electrodes in simulated corrosion and deposition experiments

3.2. Influence of pH value on the Al(III) species

Based on hydrolysis reactions, theoretical calculations for the distribution ratios of Al(III) species in valve cooling systems in engineering practice have been carried out. Figure 8 and Table 5 show the dependence of the distribution ratios of Al(III) species on the pH value, whose $c(Al)_t$ is set as 1 μg/L. In this case, the main existing forms of Al(III) species in water are five kinds of monomeric Al(III), which are Al^{3+}, $Al(OH)^{2+}$, $Al(OH)_2^+$, $Al(OH)_3(aq)$ and $Al(OH)_4^-$, as revealed in Figure 8. When the pH value changes from 3 to 9, the maximum a_i of Al(III) species in the cooling water are Al^{3+}, $Al(OH)^{2+}$, $Al(OH)_3(aq)$, $Al(OH)_4^-$ sequentially. Since electroneutral $Al(OH)_3(aq)$ does not take part in the sediment formation process, it is not considered in the following discussions. The main existing forms of monomeric Al(III) are electronegative $Al(OH)_4^-$ in weakly alkaline solution. Instead, electropositive monomeric Al(III) is the main existing form of Al(III) species in weakly acidic solutions. The distribution ratios of electropositive monomeric Al(III) decrease with pH value as the pH value of the solution is greater than 5, while the distribution ratio of electronegative $Al(OH)_4^-$ increases. These conclusions are in good agreement with the phenomenon that the sediment tends to deposit on the platinum electrodes connected as anodes in engineering practice whose cooling water is weakly alkaline (approximately 7.38 to 7.86). Although the stray-current corrosion of aluminium heat sinks at high potentials will produce Al^{3+} [8], they will mostly convert to electronegative $Al(OH)_4^-$ in the migration stage. Then, $Al(OH)_4^-$ will reach the platinum electrodes connected as anodes by Coulomb force. Since the environment around the anode is acidic when applying voltage to the electrodes (formation of H_3O^+) [12], the sediment forms, and the neutralization reaction occurs as follows:

$$Al(OH)_4^- + H_3O^+ \rightarrow Al(OH)_3(am) + 6H_2O \quad (10)$$

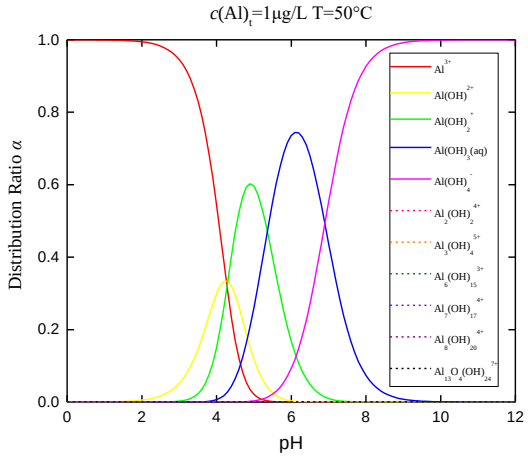

Figure 8. Dependence of distribution ratio of all Al(III) species on pH value in engineering practice: normally the temperature is maintained at approximately 50 °C， the $c(Al)_t$ is maintained at approximately 1 μg/L and the pH value is approximately 7.38 to 7.86 during normal operation

Table 5. Main existing forms of Al(III) species and their distribution ratios, in %, in engineering practice

Al^{+III} species \ pH	5.5	6.0	6.5	7.0	7.5	8.0	8.5
Al^{3+}	0.15	0	0	0	0	0	0
$Al(OH)^{2+}$	2.52	0.34	0	0	0	0	0
$Al(OH)_2^+$	39.97	16.85	4.92	0.01	0.15	0	0
$Al(OH)_3(aq)$	55.17	73.55	67.98	43.82	20.05	7.36	2.45
$Al(OH)_4^-$	2.20	9.26	27.06	55.17	79.81	92.63	97.55

Furthermore, the distribution ratios of Al(III) species in the simulated deposition experiment were also calculated, as shown in Figure 9. In general, the effect of pH on the existing forms of Al(III) species is clearly similar to the case in engineering practice. The main difference is that multimeric Al(III), such as $Al_7(OH)_{17}^{4+}$ and $Al_6(OH)_{15}^{3+}$ occur as $c(Al)_t$ increases. Moreover, electropositive Al(III) are the main existing forms of Al(III) species in weakly acidic water. The conclusions also strongly support the phenomenon that the sediment tends to deposit on the platinum electrodes connected as cathodes in the simulated deposition experiment. The circulating water was weakly acidic in the simulated deposition experiment, as shown in Table 2. Although the alkaline corrosion of aluminium heat sinks at low potentials will produce $Al(OH)_4^-$, they will mostly transform into electropositive Al(III) species in the migration stage. Then, electropositive ions migrate to the platinum electrodes connected as cathodes affected by electric field. Since the environment around the cathode is alkaline when applying voltage to the electrodes (formation of OH^-) [12], the sediment forms, and the major neutralization reactions occur as follows:

$$Al(H_2O)_6^{3+} + 3OH^- \rightarrow Al(OH)_3(am) + 6H_2O \quad (11)$$

$$Al(H_2O)_5OH^{2+} + 2OH^- \rightarrow Al(OH)_3(am) + 5H_2O \quad (12)$$

$$Al(H_2O)_4(OH)_2^+ + OH^- \rightarrow Al(OH)_3(am) + 4H_2O \quad (13)$$

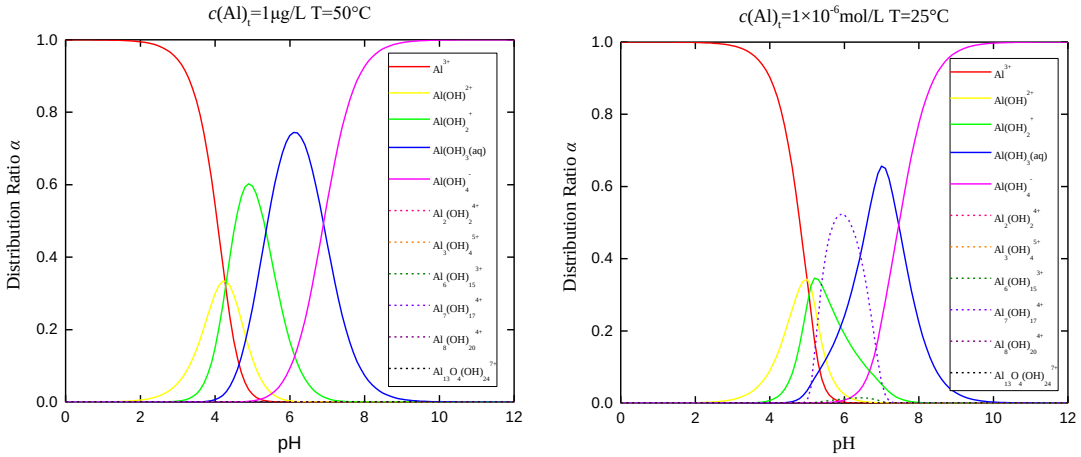

(a) case I (b) case II

Figure 9. Dependence of distribution ratios of Al(III) species on pH in simulated deposition experiment: the initial quality parameters of circulating water are given in Table 1, the pH value is approximately 6.15 and the temperature is approximately 25 °C, two cases are calculated to reveal the effect of pH value on the existing forms of Al(III) species comprehensively, (a) $c(Al)_t=1\times10^{-5}$ mol/L (270 μg/L), T=25 °C; (b) $c(Al)_t=1\times10^{-6}$ mol/L (27 μg/L)

In general, the deposition principle, which refers to the sediment tending to deposit on the platinum electrodes connected as anodes or cathodes, has a great relationship with the pH value of the circulating water in the valve cooling system. If circulating water exhibits a weakly acidic property, the aluminium corrosion products will transform into electropositive Al(III) and migrate to the platinum electrodes connected as cathodes to take part in the sediment formation process. If circulating water has a weakly alkaline property, the aluminium corrosion products will transform into electronegative $Al(OH)_4^-$ and migrate to the platinum electrodes connected as anodes to take part in the sediment formation process. Actually, it was found that in some converter stations, sediment deposition on the platinum electrodes connected as cathodes was even more serious [6,21]. The circulating water of the valve cooling system can be inferred to be weakly acidic in these converter stations. Consequently, it is necessary for maintenance personnel to monitor the pH value in valve cooling systems for HVDC converter stations, since it could help them to efficiently clear the deposition on pin-type platinum electrodes.

3.3. Deposition process on platinum electrodes

In the simulated electrode deposition experiment mentioned above, another interesting phenomenon was that the surface of cathode E_5 was completely covered by a thin and uniform deposition layer just 1 h after applying voltage, as shown in Figure 10. The sediment deposition grew slower and slower afterwards. Finally, the sediment deposition on the surface of cathode E_5 was so obvious to observe, and rod-shaped sediment deposition could stably exist in the circulating cooling water after a 120 h experiment.

(a) 0 h; (b) 1 h; (c) 12 h; (d) 24 h; (e)48 h; (f) 72h; (g) 96 h; (h) 120 h

Figure 10. Morphological changes of cathodic electrode E_5 in simulated deposition experiment

The simulation model of the single pin-type platinum electrode is shown in Figure 5. The internal diameter of water pipe is set as 57 mm. The tip of the platinum electrodes is hemispherical, and the radius is 1 mm. The immersion depth of the platinum electrodes was set as 28.5 mm. Moreover, the boundary conditions are set according to the operation parameters in converter stations. Figure 10(b) shows the electric field distribution around a single pin-type platinum electrode when the electrode current is set as 2 mA. The maximum electric field intensity is approximately 834 V/mm. The electric field is concentrated at the end of the single electrode. Moreover, the closer to the root of the electrode, the smaller the electric field intensity on the electrode surface.

(a) Platinum electrode and water circuit model (b) Electric field distribution on electrode surface

Figure 11. Simulation calculation model of single pin-type platinum electrode

Based on the theory of electrophoretic deposition, the deposition process on platinum electrodes was simulated. The simulation results are in good agreement with industrial platinum electrodes, as shown in Figure 12 (a) and (b). Clearly, the sediment deposition is rod-shaped, which means that the deposition thickness is larger at the end and thinner at the root. A possible explanation is that the sediment first deposits on the end of the electrode surface where the electric field is concentrated, as is shown in Figure 10(b). With the development of the deposition on the platinum electrode, the high resistivity of sediment deposition will force the current to gradually distribute to the place where the deposition thickness is thinner, thus increasing the normal current density of the corresponding parts. Consequently, the sediment deposition shows rod-shaped morphology.

Furthermore, the sediment deposition on the surface the platinum electrode grew continuously with increasing time, as shown in Figure 13. Analysed from a microscopic point of view, the growth of sediment is accounted in terms of the tunneling properties of protons [12]. Although it is difficult for hydrated hydroxyl complexes such as $Al(OH)_4^-$ to penetrate the deposition continuously and finally

reach the electrode surface to take part in the sediment formation reactions, protons could penetrate the thick deposition through shifting of hydrogen bonds. Moreover, the growth rate of the deposition thickness tends to decrease gradually. A possible explanation for this gradual decrease is that the high resistivity of sediment deposition will reduce the current density around the surface of pin-type platinum electrode. The simulation result is also in good agreement with the deposition phenomenon of the simulated deposition experiment, as shown in Figure 10. Based on different principles, reference [13] also studied the deposition of platinum electrodes and the results were similar. The simulation model based on electrophoretic deposition can be used to predict the growth of sediment deposition to clean the deposition on the platinum electrodes in a timely manner in engineering practice.

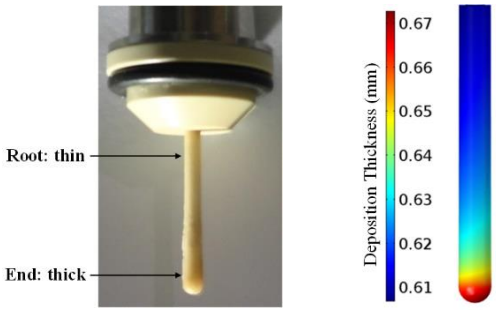

(a) Industrial sample (b) Simulation calculation

Figure 12. Sediment deposition on a single pin-type platinum electrode (in 180 days)

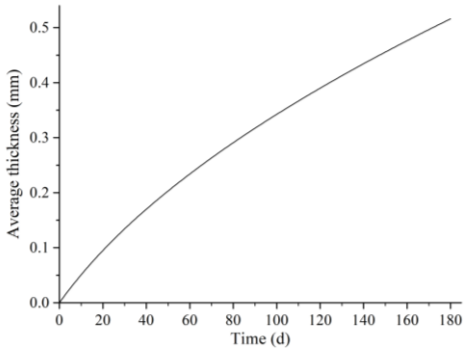

Figure 13. Average thickness of sediment deposition on a single pin-type platinum electrode vs time

4. CONCLUSIONS

In this paper, the dependence of existing forms of Al(III) species on the pH value was revealed by theoretical calculations and simulated experiments. Moreover, the simulation model based on electrophoretic deposition was consistent with the characteristics of deposition process in the simulated experiment. The main conclusions include the following:

(1) As the circulating water in the valve cooling system exhibits a weakly acidic property, the aluminium corrosion products will mostly transform into electropositive Al(III) and then migrate to the platinum electrodes connected as cathodes to take part in the sediment formation process.

(2) As circulating water has a weakly alkaline property, the aluminium corrosion products will mostly transform into electronegative $Al(OH)_4^-$ and migrate to the platinum electrodes connected as anodes to take part in the sediment formation process.

(3) The deposition process on platinum electrodes has the following characteristics: the sediment deposition is rod-shaped, and the growth rate of the deposition thickness tends to decrease gradually. Moreover, the deposition model based on electrophoretic deposition has good agreement with the deposition process in the simulated deposition experiment.

The effect of the pH value on the existing forms of Al(III) species proves that it is significant to monitor the pH value of the circulating water in valve cooling systems for HVDC converter valves, since it can help maintenance personnel clean the deposition on the platinum electrodes efficiently and improve the security of the converter valve. Furthermore, the simulation model based on electrophoretic deposition can be used to predict the growth of deposition on the platinum electrodes, thus reducing the maintenance costs and time in engineering practice.

ACKNOWLEDGEMENTS
This work was supported by the Programs of the China Southern Power Grid (CGYKJXM20180394) and Xi'an XD Power Systems Company Limited.

References

1. M. P. Bahrman and B. K. Johnson, *IEEE Power Energy Mag.*, 5 (2007) 32.
2. J. D. Páez, D. Frey, J. Maneiro and P. Dworakowski, *IEEE Trans. Power Deliv.*, 34 (2019) 119.
3. Y. Wen, M. Leng, E. Zhang, Z. Zhang and J. Chen, *Appl. Mech. Mater.*, 3391 (2014) 588.
4. H. P. Lips, *IEEE Trans. Power Deliv.*, 9 (1994) 1830.
5. Y. Wang, Z Hao and R Lin, *High. Voltage. Eng.*, 32(2006) 80.
6. X. Li, D. Ding, L. Wang and L. Sun, *IOP Conf. Ser.: Mater. Sci. Eng.,* 474 (2019) 012017.
7. C. Wang, X. Liu, X. Wang, N. Liu, X. Jiao and Y. Tan, The distributing characteristics of sediment deposited on pin-type grading electrodes in inner cooling circuit of HV converter valve, IEEE Electrical Insulation Conference, Seattle, United States, 2015, 24-28.
8. X. Liu, C. Wang, N. Liu and X. Jiao, *Corros. Eng. Sci. Technol.*, 54 (2019) 131.
9. X. Liu, C. Wang, N. Liu, X. Jiao, *High. Voltage. Eng.*, 46 (2020) 1781.
10. X. Jiao, C. Wang, X. Liu, N. Liu, L. Liu and X. Wang, *High. Voltage. Appar.*, 54 (2018) 65.
11. X. Wang, X. Liu, C. Wang, N. Liu, X. Jiao and L. Liu, Numerical calculation of current through grading electrodes in inner cooling circuit of HV converter valve, IEEE Conference on Electrical Insulation and Dielectric Phenomena, Toronto, Canada, 2015, 411-414.
12. I. Weber, B. Mallick, M. Schild, S. Kareth, R. Puchta and R. van Eldik, *Chem.-Eur. J.*, 20 (2014) 12091.
13. B. Gao, T. He, F. Yang, C. Liu, X. Song and Y. Cheng, *IEEE Access*, 7 (2019) 67960.
14. X. Song, Y. Cheng, B. Gao, Y. Fan, T. He and J. Ran, *J. Eng.*, 2019 (2019) 3396.
15. X. Wang, X. Liu and C. Wang, Research on mechanism and suppression of sediment deposition on grading electrodes in cooling water dielectric of HV converter valve, IEEE 3rd International Conference on Dielectrics, Valencia, Spain, 2020, 293-296.
16. D. Li, Y. Shi, H. Xu, Y. Chen, P. Zhou, X. Li, W. Feng and S. Wang, *Int. J. Electrochem. Sci*., 13 (2018) 9346.

17. D. Li, Y. Shi, H. Xu, Y. Chen, P. Zhou, X. Li, W. Feng and S. Wang, *Int. J. Electrochem. Sci*., 14 (2019) 3465.
18. D. Li, Z. Shi, H. Xu, Y. Chen, W. Feng, Z. Qiu, H. Liu, G. Lv, S. Wang and Y. Fan, *Int. J. Electrochem. Sci*., 15 (2020) 5320.
19. J. Y. Bottero, J. M. Cases, F. Fiessinger and J. E. Poirier, *J. Phys. Chem.*, 84 (1980) 2933.
20. C. F. Baes and R. E. Mesmer, The hydrolysis of cations, John Wiley & Sons, (1976) New York, United States.
21. D. Ding, K. Zuo, Y. Gu, X. Liu, S. Sun, J. Wu, *Clean. World*., 30 (2014) 15.